Sensors & Actuators: B. Chemical 271 (2018) 24–32

Contents lists available at ScienceDirect

Sensors and Actuators B: Chemical

journal homepage: www.elsevier.com/locate/snb

Highly sensitive label-free antibody detection using a long period fibre grating sensor

LiangLiang Liu[a], Leonel Marques[a], Ricardo Correia[a], Stephen P. Morgan[a], Seung-Woo Lee[c], Paddy Tighe[b], Lucy Fairclough[b], Serhiy Korposh[a,*]

[a] Optics and Photonics Group, Faculty of Engineering, University of Nottingham, University Park, Nottingham, UK
[b] Division of Infection, Immunity and Microbes, School of Life Sciences, Faculty of Medicine and Health Sciences, University of Nottingham, Nottingham, UK
[c] Graduate School of Environmental Engineering, University of Kitakyushu, Kitakyushu, Japan

ARTICLE INFO

Keywords:
Long period gratings
Biosensor
Layer-by-Layer techniques
Optical fibre sensor
Streptavidin
Human IgM

ABSTRACT

An optical fibre long period grating (LPG) biosensor is appealing in the detection of biomolecules because of the high sensitivity, label-free and real-time measurement. The miniaturized size, ability of remote sensing and immunity to electromagnetic interference of the LPG biosensor provide various possibility of single-point sensing in situations such as point of care diagnostics and *in vivo* measurement. Two optical fibre LPG based biosensors are reported for detection of streptavidin (SV) and immunoglobulin M (IgM) respectively. The LPG is coated with a film containing three layers of Poly(allylamine hydrochloride)/gold coated silica nanoparticles *via* the layer-by-layer method. Biotin is covalently bonded to the surface of the gold shell by means of the formation of an amide bonds for detection of streptavidin. The concentration of SV in water for detection varied from 1.25 nM to 2.7 μM. The LPG sensor, operating close to the phase matching condition shows a high sensitivity of 3.88 $(ng/mm^2)^{-1}$ and a detection limit of 0.86 pg/mm^2 for the detection of SV. The limit of detection is 22 times lower than previously demonstrated with this type of sensor. The developed IgM sensor has the same configuration of film but has anti-IgM embedded on the LPG instead of biotin, demonstrating versatility of the sensing platform. This was used for the detection of human IgM with concentrations from 15.6 μg/ml to 1 mg/ml. The LPG sensor exhibits a sensitivity of 11 nm $(ng/mm^2)^{-1}$ for the detection of IgM with a detection limit of 15 pg/mm^2. The developed highly sensitive IgM sensor shows the potential application of clinical point of care for detection of lower concentration of IgM *in vitro*. The proposed biosensor exhibits high sensitivity and rapid detection of low concentrations biomolecules from the small size of SV to the large size of IgM.

1. Introduction

Antibodies/antigens are important biomarkers in human body fluids. They participate in the humoral immune response and their levels increases during the immune system responses to pathogen infection. The level of antibody/antigen can be used as an indicator of infectious disease [1]. Immunoglobulin M (IgM), as the earliest antibody to appear in the course of an infection [2], is responsible for agglutination and activating cytolytic responses. The pentameric structure of IgM theoretically provides 10 free antigen-binding sites and high avidity binding. IgM is mainly found in blood and lymph fluid and it is a very effective neutralizing agent in the early stage of disease. The level of IgM has significant clinical value in diagnosis of certain diseases. For example, because IgM antibody does not cross placenta, it can indicate a recent infection or intrauterine infection when it appears in a neonate's serum [3,4]. IgM also plays a vital role in rapid diagnosis of Dengue virus infection as it appears as the initial immune response to a primary infection a few days after the onset of Dengue fever [5]. In addition, IgM regulates autoimmunity and atherosclerosis and deficiency of IgM indicates increased susceptibility [6]. Selective IgM deficiency (SIgMD) is an immune disorder that is associated with serious infection. The deficiency of IgM in blood, usually < 20 mg/dl, can develop to prolonged or life-threatening infection to the patients (often infants and small children). The common method used in clinical practice for detection of antigens or antibodies is based on the enzyme-linked immunosorbent assay (ELISA) [7]. Dependent on the exact method used, the technique usually involves multiple sequential incubations for long periods (60–90 min each) and multiple wash steps, resulting ultimately in a colorimetric readout which is proportional to the level of the antigen or antibody present in the original sample. The readout requires a dedicated optical plate reader for translating the readings. Moreover, the multi-step nature of the procedure and

* Corresponding author.
E-mail address: s.korposh@nottingham.ac.uk (S. Korposh).

https://doi.org/10.1016/j.snb.2018.05.109
Received 9 November 2017; Received in revised form 10 May 2018; Accepted 18 May 2018
Available online 19 May 2018

requirement for enzyme-labelled antibodies is a significant weakness and does not allow real time detection of target molecules. Fast and accurate detection of IgM in patients' serum would enable early screening of SIgMD and early intervention may help prevent some of the complications seen later in life. Some infections due to the deficiency of IgM in infants and small children such as bacteremia can be life-threatening.

To satisfy the need for real time point-of-care (POC) testing, researchers have focused on the development of different protein measurement methods in order to obtain accurate, fast sensors that would be able to replace the current ELISA method. Surface Plasmon resonance (SPR) has been extensively used for quantitative measurement with sensitivity of the order of μg/ml [8]. However, a drawback is the relatively high price and bulky optical system that usually limits its application to the clinical laboratory. Quartz crystal microbalance (QCM) [9] is also an important label-free method for the detection of antibodies. The shift of resonance frequency is induced by the mass change of crystal resonator after binding of antibodies. However, the viscosity of analysed liquid also contributes to the frequency shift. In order to distinguish the mass-affected frequency shift with the contribution of liquid, a more expensive impedance analyser is required. A hybrid whispering gallery mode sensor [10] has been used for detection and characterization of small molecule such as RNA viruses, however, the lack of a bio-receptor makes the sensor non-specific in terms of biomolecule detection. Flow cytometry [11,12] has been used for the detection of antibodies. The techniques can be used for detection of antibodies which are not be detected by ELISA (*e.g.* glycospecific antibodies). However, the technique is not widely used due to the high cost compared with other alternatives. Planar waveguide sensors are also widely applied in detection of biomolecules [13]. The performance of this type of sensor strongly relies on the choice of substrate material and the quality of the deposited film. Fluorescence has been used for detection of nucleic acid on planar optical waveguides [14]. The use of fluorescent labels in the context of planar optical waveguide allows better sensitivity and specificity. The disadvantages of fluorescence detection include the rapid photo bleaching of fluorescent dyes conjugated to the biomolecules of interest and the potential loss of activity of the biomolecules when chemically conjugated with fluorescent dyes.

To satisfy the requirements of POC devices, it is not only sensitivity and response time that have to be taken into account, but also the size and simplicity of the sensor. In this regard, an optical fibre based sensor, due to its small size, provides an advantage in terms of application in point of care devices used in the clinic or community. In addition, the optical fibre is immune to the interaction of electromagnetic field providing a robust response in environments containing electronic devices.

A long period fibre grating (LPG) is a refractive index grating inscribed in the fibre's core. The theory of operation of LPG and biosensor parameters used in this work can be found in Supporting information (SI). This enables light to be coupled into the cladding region and produces characteristic attenuation bands in the transmission spectrum of the optical fibre [15]. A LPG is sensitive to the refractive index (RI) of the cladding region and therefore bio-sensing can be achieved by modifying the outside of the cladding with a functional material whose RI changes in the presence of an analyte of interest. Sensors based on LPGs have been reported for measurement of pH [16], detection of bacteria [17] and virus [18] after modifying the LPG with corresponding functional materials. The RI sensitivity of LPGs has been reported as high as 10^{-6} [19] offering the potential for bio-molecule detection. This removes the need for enzyme labelling and provides label free, low cost, rapid, point of care detection of bio-molecules.

The optimum functional coating combines high sensitivity and high specificity. Silica nanoparticles, due to their high surface to volume ratio can be incorporated into the coating film of LPG and significantly raise the RI sensitivity of the LPG [20]. Gold nanoparticles, due to their unique optical and electrical property, are commonly applied in the sensor development [21–23]. The localized surface plasmons are generated near the gold nanoparticles surface and enhance the overall electromagnetic field which leads to an increase in sensitivity. In our previous work we have developed [22] a LPG bio-sensor modified with poly(allylamine hydrochloride)/silica core gold shell nanoparticles for detection of the streptavidin with a high sensitivity (6.9 nm/(ng/mm^2)) and the minimum detectable concentration of 19 nM. However, the sensor performance was not optimal due to the poor surface coverage and uniformity of the coating. In addition, selected grating period of the LPG sensor was near rather than at the phase matching turning point (PMTP) which also did not lead to the optimal performance.

In this work, we address these points in order to fully realise the optimum performance of these sensors. In particular, a new approach of functionally coating the LPG is reported in order to provide significantly improved sensitivity (minimum detectable concentration of 1.25 nM for streptavidin compared to 19 nM previously [22]). Silica nanoparticles are first deposited onto the LPG using the layer-by-layer method in order to address the surface coverage problem providing a more uniform surface coverage. The surface of the silica particles is then further modified with 3-aminopropyltriethoxhysilane (APTES) *via* a silanization process in order to covalently attach gold nanoparticles (diameter of 2–5 nm) to the silica nanoparticles, forming a shell structure *via* a chemisorption process. In addition, chemical linkers are applied to covalently link the gold nanoparticles and the bio-receptor in order to minimize unspecific binding to the gold surface. Crucially the LPG sensor is fabricated close to the phase matching condition and, at the deposition of sensing film, the coupling conditions are modified such that sensors operate at the highly sensitive PMTP. The transmission changes at a specific wavelength, corresponding to the resonance band at the PMTP, are detected which has been reported to be more sensitive than the wavelength shift [24]. After optimising the LPG sensor performance using SV, it was then used to detect human IgM by functionalizing the coated LPG with anti-human IgM antibody as a proof of concept for application in clinical point of care.

2. Method

2.1. LPG modification

2.1.1. Modification for streptavidin detection

A list of materials used in this work can be found in SI section 1.3. The LPG was coated with three layers of silica nanoparticles (SiNPs) using the layer-by-layer method [19]. A positively charged polymer, poly(allylamine hydrochloride) (PAH) and negative charged SiNPs were subsequently deposited on the surface of the LPG *via* electrostatic interaction for three cycles as illustrated in Fig. 1a. The SiNPs coated on the LPG were then further decorated with an amine group using APTES to covalently attach gold nanoparticles and detailed description of this procedure is described in SI, section 1.4.

2.1.2. Modification for IgM detection

A three layer silica-Au coated LPG was fabricated using the assembly method by immersion into 20 mM 11-Mercaptoundecanoic acid (11-MUA) solution in ethanol for 30 min. The self-assembled monolayer of the thiol linkers in 11-MUA solution made a continuous binding to the gold surface leading to a termination of −COOH group. The LPG was then immersed into 25 mM EDC solution in MES buffer (0.1 M pH = 5.6, with 0.9% NaCl) for 20 min followed by immediately immersion in 60 mM NHS solution (0.1 M PBS buffer, pH = 7.4) for another 20 min. After brief washing with deionized water, the LPG was immersed into a solution that contains 1 mg/ml anti-IgM in PBS buffer for 1 h at room temperature (temperature regulated at 26 °C). The schematic of the modification is illustrated in Fig. 2.

After washing with deionized water, the anti-IgM functionalized sensor was then immersed into 1 mg/ml BSA for incubation of 1 h in room temperature followed by washing with deionized water to remove

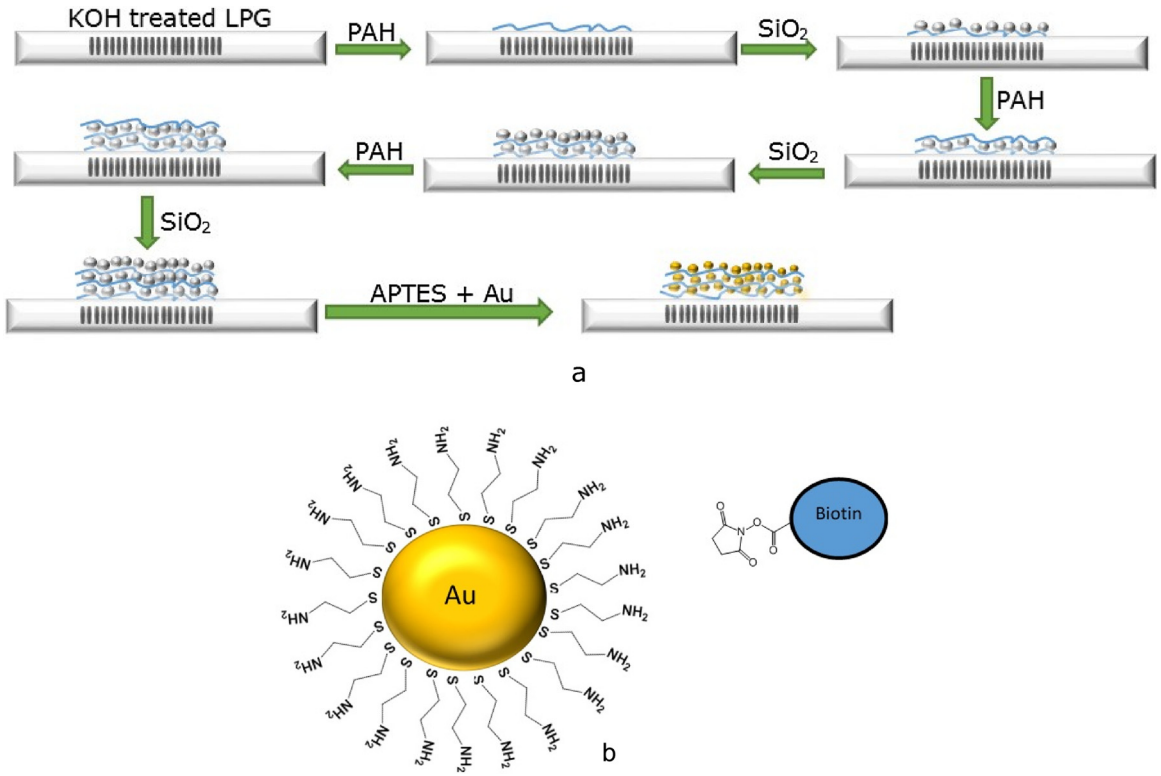

Fig. 1. (a) Schematic diagram of the layer-by-layer modification of LPG. The bare LPG was initially treated with KOH to etch −OH group, and then followed by subsequently adding polycations (PAH) and negatively charged SiNPs to build up the film layer-by-layer. The functionalisation of silica nanoparticles was achieved by APTES with a silanization process for attachment of gold nanoparticles forming a shell structure. (b) Gold nanoparticle chemically decorated with amine groups to attach biotin.

excess unbound proteins.

2.2. Characterisation experiments

Prepared nanoparticles and fabricated thin films were characterised using Malvern Zetasizer Nano-ZS (Malvern Instruments, UK), transmission electron microscopy (TEM) (JEM-3010, JEOL, Japan) and scanning electron microscopy (JSM-7100F, JEOL, UK). After sensor functionalisation it was exposed to aqueous solutions containing streptavidin or human IgM antibodies. Detailed description of sensors characterisation and the experimental protocol can be found in SI, section 1.5.

2.3. Experimental set-up

The coated LPG of length 3 cm, period 110 um and duty cycle of

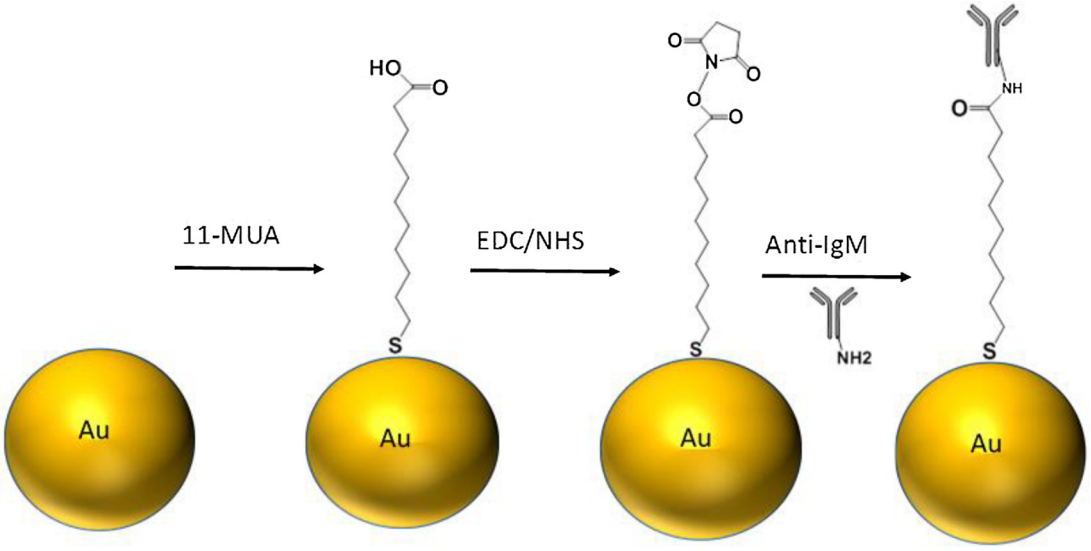

Fig. 2. The modification of LPG for the detection of IgM. The LPG has been coated with three layer PAH/SiNPs-Au in advance as illustrated as Fig. 1(a). Then an EDC/NHS linker is activated and linked on the surface of gold *via* a two-step procedure. The primary amine group of anti-IgM covalently binds to the activated NHS esters leading to the immobilisation of anti-IgM on the LPG sensor.

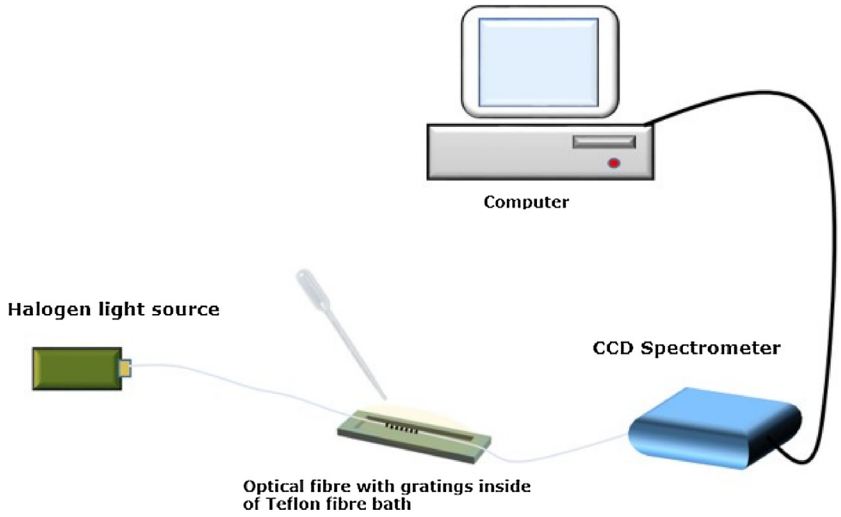

Fig. 3. LPG sensor set-up.

50:50 was inscribed into a boron-germanium co-doped single mode silica fibre (Fibrecore, PS750, UK) by ultraviolet (UV) exposure through an amplitude mask [25]. The UV source is a frequency-quadrupled Nd:YAG laser operating at a wavelength of 266 nm. The amplitude mask with a period of 110 um was made of steel (1Cr18Ni9Ti, Suzhou Sunshine Laser Technology, China)

The LPG sensor region was placed into a Teflon fibre bath (inner well diameter: 55(L) × 5(W) × 4(D) mm) containing the solution under test (Fig. 3) for SV detection and IgM detection. The proximal and distal end of the optical fibre were connected to a Halogen light source (Ocean optics, HL-2000, UK) and CCD spectrometer (Ocean optics, HR4000, UK) respectively with data transferred to a computer for post processing.

3. Results and discussion

3.1. LPG characterisation

Fig. 4a shows that the size of the prepared silica nanoparticles varies from 68 to 295 nm with an average diameter of 137 ± 46 nm and a mode diameter of 151 nm. The polydispersity index (PDI) is 0.08. The TEM image of SiNPs coated with a gold shell is shown in Fig. 4b. The image confirmed the successful deposition of gold nanoparticles onto the coated SiNPs. A film containing three layers of PAH/SiNPs with gold coated on the surface was deposited onto the optical fibre and its SEM results are shown in Fig. 4c indicating a good surface coverage. The thickness of three layers on the optical fibre is measured as 863 nm from the SEM image in Fig. 4d. The film thickness of three layers film is more than twice of the expected thickness based on the nanoparticles diameter (414 nm, neglecting the contribution of PAH). This can be attributed to the high concentration of silica nanoparticles that leads to the strong ionic interaction or the aggregation of silica nanoparticles on PAH film [26].

The deposited film increases the RI probed by the LPG leading to a shift in the position of the attenuation bands. As illustrated in Fig. 5a, the attenuation band corresponding to coupling of the 18th linearly polarised mode (LP_{018}) undergoes a blue-shift in response to each layer deposited and LP_{019} with a centre wavelength of 850 nm starts to appear as a wide attenuation band that further grows as each layer is deposited. The attachment of gold nanoparticles can also be observed in the transmission spectrum which causes a further increase in attenuation. Since the sensitivity of LPG sensor to ambient RI change is thickness-dependent [27], the sensor was coated with 6 layers of PAH/SiNPs thin film (Fig. 5b). As can be observed from Fig. 5b, the slope of wavelength decreases after 3 layers confirming that the optimal thickness of the PAH/SiNPs thin film is reached after 3 deposited layers, corresponding to ca 900 nm (Fig. 4d).

The sensor optimization in terms of the size of silica nanoparticles was investigated in our previous work [22] where the large particles (300 nm) exhibit a higher sensitivity than the small one (80 nm) because of the higher efficiency of evanescent wave interaction and larger pore size that allows more efficient adsorption of proteins. However, due to the limitation of surface coverage encountered using large size nanoparticles, the particles with average size 137 nm (mode diameter: 151 nm) were used in this work to improve the coverage while maintaining the benefits of larger particles. The concentration of gold nanoparticles was chosen such that the shell structure illustrated in Fig. 4b can be produced.

To avoid the effect of the bulk reflective index change in different solutions during the deposition process, spectra were always measured and then compared with water. This takes into account the signal change caused only by the specific binding. For binding measurements, the RI of the blank sample and target samples were measured using a refractometer and no detectable change was measured.

3.2. Streptavidin detection

The modified LPG was first immersed into a biotin solution with concentration of 1 mg/ml (2.9 mM). The biotin molecules start to react with $-NH_2$ group of the gold nanoparticles. The bound biotin molecules on LPG surface increase the RI of the film coated on the LPG, which leads to a wavelength shift of 0.5 nm for LP_{018} mode and a transmission change of an approximate 7% (0.06988) for LP_{019} mode (Fig. S1). The wavelength shift induced by the bonded biotin at the first attenuation band (LP_{018}) is bigger than determined previously [22] (0.11 nm).

Streptavidin (SV) has very high affinity of binding to biotin [28] and is known as the strongest noncovalent interaction between proteins and ligand [29]. One SV molecule has the ability to bind with up to four biotin molecules. The bond formation between biotin and streptavidin is rapid (in a range of 3.0×10^6–$4.5 \times 10^7\ M^{-1} s^{-1}$) [30].

The attenuation band at 850 nm (LP_{019} centre wavelength) becomes bigger and broader with increasing SV concentration Fig. 6a. The optical transmission measured at 850 nm show a step change with increasing of streptavidin concentration (illustrated in Fig. 6b). The transmission value at this wavelength in air equals to 1 indicating that the sensor is not at phase matching condition when operating in air due to lower RI of air ($n_{air} = 1$) when compared with the aqueous solution. The refractive index of the tested SV solution measured with a refractometer showed the same value as deionized water (1.3330). Therefore, the contribution of bulk RI caused by different SV

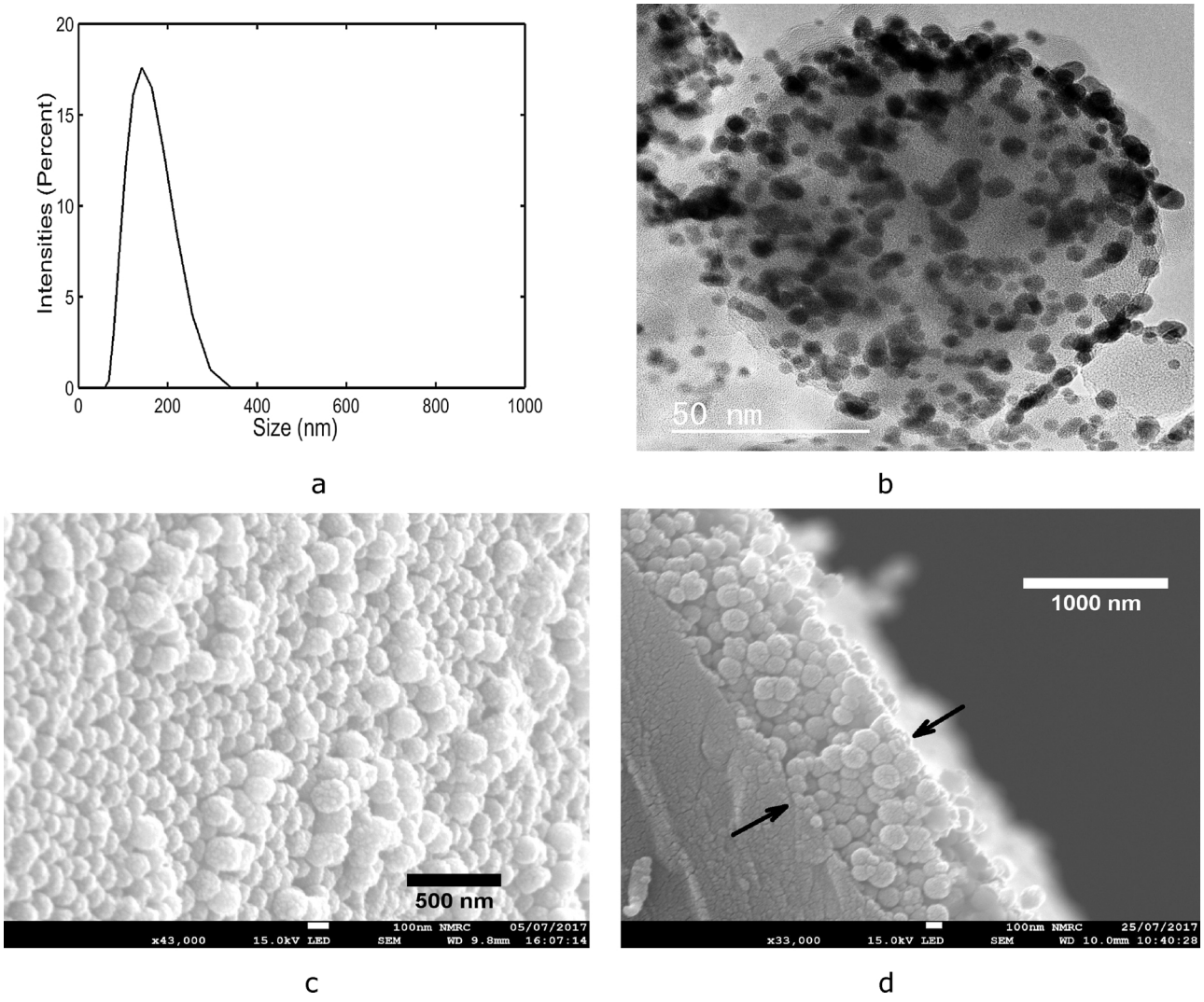

Fig. 4. (a) DLS measurement of the size (diameter) distribution of SiNPs with peak at 151 nm (b) TEM image of SiNPs with gold shell, the particles were scratched from the coated glass substrates confirming the attachment of gold nanoparticles with the shell structure (scale bar = 50 nm). (c) SEM of three layers of PAH/SiNPs with gold shell (scale bar = 500 nm). (d) Cross-section of optical fibre with three layers of PAH/SiNPs with gold shell (scale bar = 1 μm). The arrows illustrate the thickness of the film, measured as 863 nm.

concentrations is negligible. For the lower concentration of SV (up to 19 nM), the response time of the sensor is less than 10 min and binding events between biotin and streptavidin were finished after 20 min. For the concentration above 19 nM, the sensor shows dynamic change of transmission indicating the binding of streptavidin. The slope of the transmission signal increases with increase of streptavidin concentration. This is attributed to the higher association ratio of the binding reaction caused by the higher concentration of reactant (SV). The change of transmission signal at higher concentration (83 nM to 2.7 μM) did not stop within the observed 20 min and also shows no saturation at the extended 10 min. During the one hour reaction at concentration of 2.7 μM, the transmission signal shows gradual

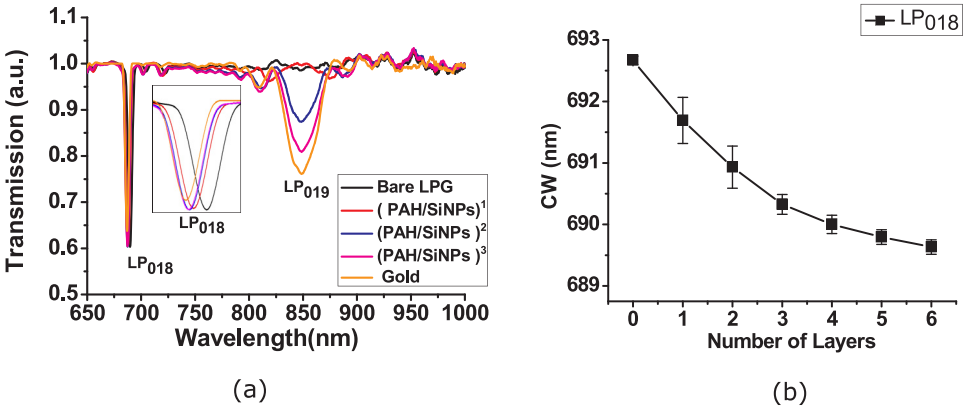

Fig. 5. (a) Transmission spectra of LPG in water after deposition of $(PAH/SiNPs)^n$ film (n = 1–3 layers) and gold. Centre wavelength of LP_{018} shifts to the left with each layer deposition process and the transmission of attenuation band at LP_{019} decreases with increasing of layers. (b) The centre wavelength (CW) of LPG at LP_{018} in water as a function of layers. The error bars represent the standard deviation between two times repeated deposition process.

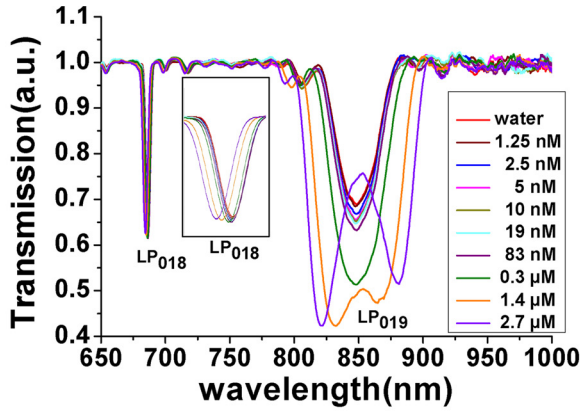

(a)

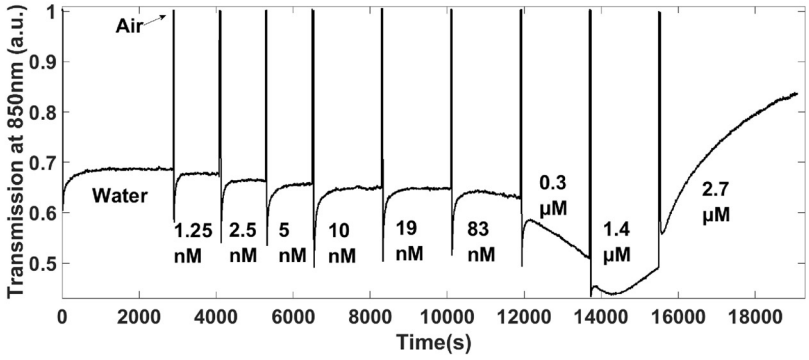

(b)

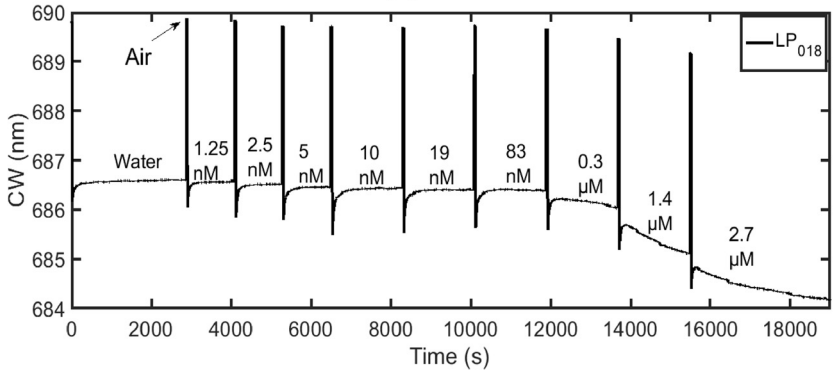

(c)

Fig. 6. (a) Transmission spectrum of the LPG in different concentrations of streptavidin solution. (b) The transmission value at wavelength of 850 nm of LP_{019} against time during measurement; the signal was recorded continuously for each measurement of concentration, excluding the wash steps. (c) The wavelength shift of LP_{018} against time during measurement.

saturation of signal indicating the ending of binding events. The transmission intensity value starts to increase at a concentration of 1.4 μM due to further development of the attenuation band at LP_{019} and it splits into two coupled bands moving in opposite directions as the RI increases, resulting in an increase of the transmission intensity value (illustrated in Fig. 6a).

The theoretical value of transmission signal of the sensor is calculated using Eq. (2), SI. The value of parameters (k, M and β) are defined by the means of nonlinear least-squares data fitting [31,32]. From the calculation based on Solver [31], the best fitting is achieved when the parameters are set as k = 0.000001, M = 24.8617 and β = 0.660836, respectively. Thus, the maximum transmission change and binding constant are 24.8617 and $0.001(pM)^{-1}$. Fig. S1b shows that the transmission change at the centre wavelength (850 nm) after 20 min reaction fits to the Langmuir-Freundlich isotherm. The coefficient of determination $R^2 = 0.9899$, $p < 0.05$.

As described in [22], the theoretical surface density of a streptavidin monolayer is 6.4 ng/mm^2 making the sensitivity of the LPG sensor = 3.88 $(ng/mm^2)^{-1}$ based on the calculation from (4), SI. The resolution of the system is defined by the noise level in the blank measurement which is the fluctuation of transmission at central wavelength (850 nm) in water measurements (Fig. 6b). The system resolution is two times the standard deviation of the stabilized transmission signal in water (2 × 0.00167 = 0.00334). The theoretical limit of detection of the sensor is then calculated as 0.86 pg/mm^2.

The central wavelength at LP_{018} continuously shifts to a lower wavelength as the concentration of SV increases. The dynamic binding can be observed in the same concentration range as the transmission value at LP_{019} (Fig. 6c). Fig.S1b illustrates wavelength shift of LP_{018} attenuation band after 20 min reaction at each concentration and its

Table 1
Comparison of developed sensor with sensor in [22].

References	Type of sensor	Type of film	Uniformity of film	Type of protein detection	Limit of Detection
Marques et al. [22]	LPG sensor at PMTP (Wavelength shift)	Silica core gold shell nanoparticles	Poor	Biotin-streptavidin	19 pg/mm^2
Developed sensor	LPG sensor close to PMTP (Change of transmission)	Silica core gold shell nanoparticles	Good	Biotin-streptavidin	0.86 pg/mm^2

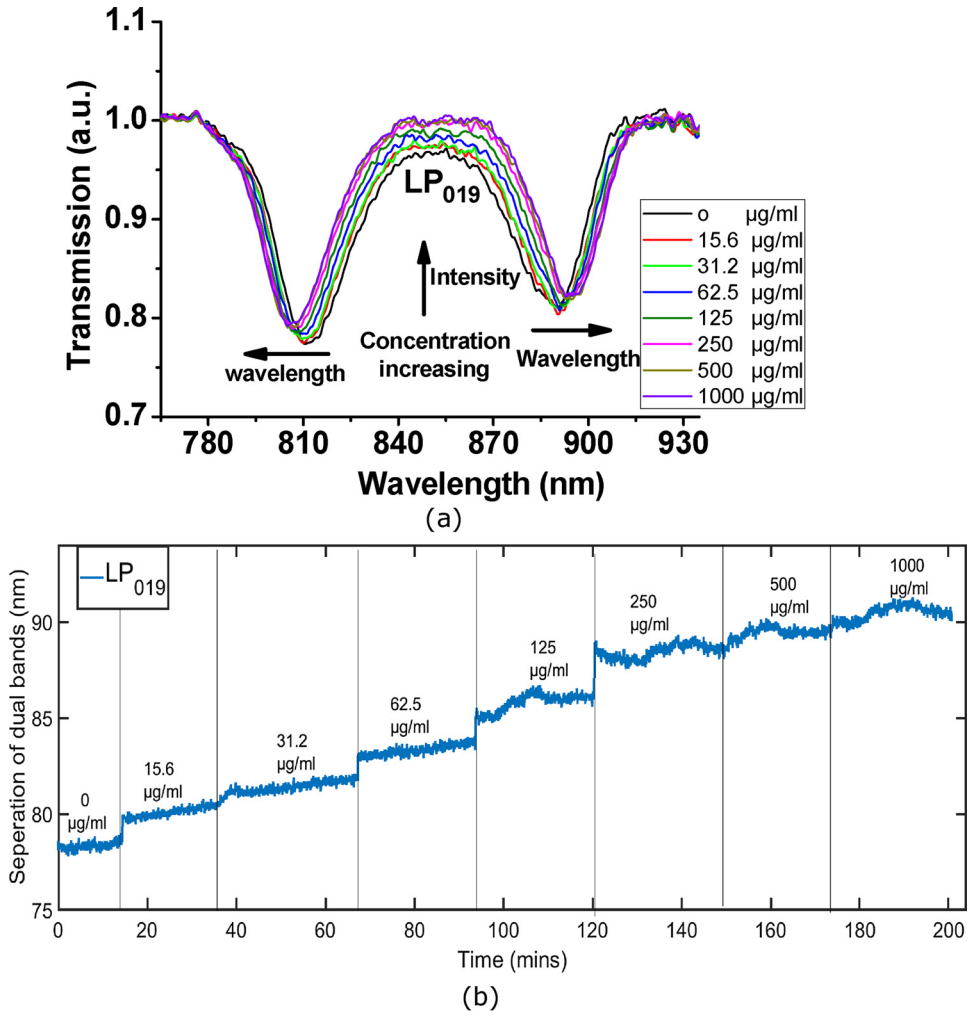

Fig. 7. (a) Transmission spectrum of the LPG in different concentrations of IgM. (b) The separation of dual bands at LP_{019} in response to different concentrations of IgM suspension solution.

Table 2
List of biosensors for the detection of IgM.

Reference	Type of sensor	Analyte(target)	Sensitivity	Limit of detection
Wong et al. [36]	Surface Plasmon waveguide	IgM antibody	N/A	12 pg/mm^2
Atias et al. [37]	chemiluminescent optical fibre immunosensor (OFIS)	IgM antibody	98.1%	1:10^6 dilution
Choi et al. [38]	Giant Magnetoresistance (GMR)	IgM antibody	50 ng/ml	N/A
Developed sensor	LPG sensor	IgM antibody	11 nm/(ng/mm^2).	15 pg/mm^2

Langmuir-Freundlich isotherm. The analysis of LP_{018} revealed the same binding constant of 0.001(pM)$^{-1}$ as compared with the LP_{019} and a maximum wavelength shift of 92.3 nm. The sensitivity and limit of detection are then calculated as 14.04 nm/(ng/mm^2) and 12.1 pg/mm^2, respectively. The sensitivity of the lower cladding mode LP_{018} is also higher than the highest sensitivity reported in [22] by using the cladding mode LP_{019} (6.9 nm/(ng/mm^2)). Although the limit of detection when wavelength shift is considered is higher than intensity measurements, the former does not require intensity reference measurements and also with the use of reference grating can account for any temperature fluctuations

Table 1 lists the LoD values between this sensor and the sensor reported by [22]. Compared with the previous sensor reported by [22], the developed sensor has higher sensitivity (3.88 (ng/mm^2)$^{-1}$) and 22 times lower limit of detection. The main reason of higher sensitivity is attributed to the optimisation of the sensor parameters such as grating

period and film coverage.

The reproducibility of the LPG sensing platform performance relies on the precise fabrication of LPG sensor and functionalization process that allow the sensor to operate at or close to the phase matching condition. This can be achieved by tightly controlling the laser fabrication process of the LPG sensor [25] and an automation based functionalization process that help to reduce the variation of each sensor from manual production of the functional coating by the strict control of the immersion time, wash step and drying process [33].

3.3. IgM detection

Attachment of anti-IgM on the surface of the LPG sensor caused a change of RI of the coating leading to a total wavelength shift of 8.57 nm in LP_{019}, Fig. S2a. The wavelength shift at the LP_{019} during the binding of anti-IgM in the solution was observed as a gradual saturation within the 1 h immersion time.

Different concentrations of IgM (from 15.6 μg/ml (16.42 nM) to 1 mg/ml (1 μM) were detected. The central wavelength of LP_{019} (at 850 nm) undergoes an increase in transmission value and the separation of dual bands at LP_{019} gets wider as increasing the concentration (Fig. 7a). Fig. 7b shows the separation of dual bands at LP_{019} with time during the measurement of different concentrations of IgM. The data of washing steps and immersing process are excluded. The LPG sensor exhibits the immediate response in the presence of IgM in solution. The dynamic binding process can be observed from each concentration as the wavelength separation of dual bands start to increase during immersion time of each concentration. A fast binding and the gradual saturation of signal are observed in higher concentration (≧125 μg/ml) which indicate the gradual saturation of available binding sites on the sensor surface.

The shift of wavelength at LP_{019} mode introduced by each concentration of IgM fits well to the applied Langmuir-Freundich isotherm by using the method demonstrated in 4.2 with coefficient of determination value $R^2 = 0.9965$ (Fig. S2b) ($p < 0.05$). The heterogeneity parameter $\beta = 1$ in Eq. (2) and the fitting becomes the Langmuir isotherm. The binding constant and maximum wavelength shift are determined as 0.012 $(\mu g/ml)^{-1}$ and 13.72 nm, respectively. The theoretical surface density of an IgM monolayer is 1.26 ng/mm^2 based on the average size of IgM reported by [34] and [35]. Thus, the sensitivity of the LPG for IgM detection is calculated as 11 nm/(ng/mm^2) based on Eq. (4), SI. The resolution of the spectrometer is 0.17 nm, thus the limit of detection is calculated as 0.015 ng/mm^2.

The RI of IgM solution (1 mg/ml) is measured as 1.3365 which shows no detectable RI difference compared with the blank sample (buffer solution). Therefore, the signal change contributed by the different RI of each tested solution is negligible. The specific binding of anti-IgM with IgM ensures the high specificity of the developed sensor for detection of IgM. BSA was used as an agent to block the potential unspecific binding of biomolecules on gold nanoparticles surface. As a control, the prepared IgM sensor was tested in a 1 mg/ml BSA solution that revealed a total shift of 1.14 nm in wavelength (Figs. S2b and S3) (most likely due to bulk RI change due to very high concentration) which is smaller than the contribution of any tested IgM concentration confirming the specific response of developed sensor to the human IgM.

Table 2 shows the comparison of the developed LPG IgM sensor with other reported IgM biosensors. The developed LPG sensor has comparable performance in terms of sensitivity and the limit of detection compared with other types of sensors including SPR [36], Chemiluminescent sensor [37] and Giant Magnetoresistance sensor [38]. However, among these types of sensors, the LPG sensor is the only one that is low cost, high sensitivity and has label free operation. The IgM levels reported in adults and children with SIgMD are 29.7 ± 8.7 mg/dl (mean ± SD) and 16.5 ± 13.8 mg/dl (mean ± SD) [39,40]. In the developed sensor, the concentration range detected is from 1.56 mg/dl to 100 mg/dl. The developed sensor exhibited the capability of detecting IgM levels in a wide range concentrations and is useful in screening SIgMD (< 20 mg/dl) and diagnosis of neonatal infection (> 20 mg/dl). Also the ability of dynamic monitoring the binding process supports the application of the sensor in POC diagnostics.

For IgM detection, the LPG with the same grating period and coating thickness as for SV detection is used. However, the IgM experiment is conducted in buffer solution with slightly higher RI (1.3365) than the water (1.3330) used in SV experiment causing the change in transmission spectrum. The limit of detection when using the transmission of the centre wavelength as signal (as described in section 4.2) is 97 pg/mm^2 which is higher than the value of wavelength shift (15 pg/mm^2), consistent with the SV measurements.

In order to achieve the optimal phase matching condition, the grating period of LPG sensor, sensor functionalization process as well as the working environment such as solvent of target molecules; and temperature of sample need to be taken into account when designing such a biosensor. Among those parameters, the layer-by-layer coating process described in the paper is a reliable and repeatable coating process. If the working environment parameters (*e.g.* RI and temperature) are known, the optimal sensor performance can be achieved by designing the precise grating period of the LPG sensor based on the provided working environment parameters. The results presented in the paper were achieved in a temperature regulated lab condition in which the temperature cross-sensitivity is neglected (according to the measured data Fig. S7). However, in the practical application, the temperature effect will always need to be taken into account. A reference LPG sensor can be added to compensate the temperature effect as well as the bulk RI induced signal change [41].

4. Conclusion

A LPG optical fibre based sensor coated with a film comprising three layers of PAH/SiNPs with gold shell for detection of streptavidin and IgM was constructed. The data of binding events fits the Langmuir isotherm. The LPG sensor operating close to the phase matching condition shows a high sensitivity of 3.88 $(ng/mm^2)^{-1}$ with a detection limit of 0.86 pg/mm^2 for the detection of SV. The minimum detectable concentration of streptavidin is 1.25 nM. The sensor performance has been improved compared to the previous best performance for this type of sensor reported by [22] (limit of detection: 19 pg/mm^2, minimum detectable concentration: 19 nM) due to the selection of the LPG sensitive working region and improvement of the uniformity of the coating surface.

The LPG sensor also demonstrates the capability of detecting human IgM with a sensitivity of 11 nm/(ng/mm^2) and detection limit of 15 pg/mm^2 in buffer solution. The low cost, real time detection, highly specificity would enable the sensor to be applied in clinical POC for the diagnosis of IgM related diseases.

Acknowledgements

This work was supported by the Engineering and Physical Sciences Research Council [grant numbers EP/N026985/1, EP/N025725/1]. LL Liu was funded by an EPSRC PhD studentship. The authors thank the Nanoscale and Microscale Research Centre (nmRC) for providing access to instrumentation.

Appendix A. Supplementary data

Supplementary data associated with this article can be found, in the online version, at https://doi.org/10.1016/j.snb.2018.05.109.

References

[1] C.A. Janeway Jr, P. Travers, M. Walport, et al., The Humoral Immune Response, 5th ed., Garland Science, New York, 2001.

[2] J.S. Fellah, M.V. Wiles, J. Charlemagne, J. Schwager, Evolution of vertebrate IgM: complete amino acid sequence of the constant region of Ambystoma mexicanum μ chain deduced from cDNA sequence, Eur. J. Immunol. 22 (10) (1992) 2595–2601.
[3] S.A. Haider, Serum IgM in diagnosis of infection in the newborn, Arch. Dis. Child. 47 (253) (1972) 382–393.
[4] D.J. Vick, W.A. Hogge, D.E. Normansell, et al., Determination of normal human fetal immunoglobulin M levels, Clin. Diagn. Lab. Immunol. 2 (1) (1995) 115–117.
[5] J.R.C. Lima, M.Z. Rouquayrol, M.R.M. Callado, M.I.F. Guedes, C. Pessoa, Interpretation of the presence of IgM and IgG antibodies in a rapid test for dengue: analysis of dengue antibody prevalence in Fortaleza City in the 20th year of the epidemic, Rev. Soc. Bras. Med. Trop. 45 (2012) 163–167.
[6] M.R. Ehrenstein, C.A. Notley, The importance of natural IgM: scavenger, protector and regulator, Nat. Rev. Immunol. 10 (11) (2010) 778–786.
[7] G.T. Hermanson, Introduction to Bioconjugation, (2013), pp. 1–125.
[8] H.H. Nguyen, J. Park, S. Kang, M. Kim, Surface plasmon resonance: a versatile technique for biosensor applications, Sensors 15 (5) (2015) 10481–10510.
[9] Y.S. Fung, Y.Y. Wong, Self-assembled monolayers as the coating in a quartz piezoelectric crystal immunosensor to detect Salmonella in aqueous solution, Anal. Chem. 73 (21) (2001) 5302–5309.
[10] S. Holler, V.R. Dantham, V. Kolchenko, Z. Wan, S. Arnold, A Hybrid Plasmonic Whispering Gallery Mode Sensor for Single Bionanoparticle Detection, (2013), p. 8722 87220T.
[11] I. Abdel-Hamid, P. Atanasov, A.L. Ghindilis, E. Wilkins, Development of a flow-through immunoassay system, Sens. Actuators B 49 (3) (1998) 202–210.
[12] C.H.M.J. Van Elssen, H. Clausen, W.T.V. Germeraad, E.P. Bennet, P.P. Menheere, G.M.J. Bos, J. Vanderlocht, Flow cytometry-based assay to evaluate human serum MUC1-Tn antibodies, J. Immunol. Methods 365 (1) (2011) 87–94.
[13] H. Mukundan, A.S. Anderson, W.K. Grace, K.M. Grace, N. Hartman, J.S. Martinez, B.I. Swanson, Waveguide-based biosensors for pathogen detection, Sensors 9 (7) (2009) 5783–5809.
[14] G.L. Duveneck, A.P. Abel, M.A. Bopp, G.M. Kresbach, M. Ehrat, Planar waveguides for ultra-high sensitivity of the analysis of nucleic acids, Anal. Chim. Acta 469 (1) (2002) 49–61.
[15] S.W. James, R. Tatam, Optical fibre long-period grating sensors: characteristics and application, Meas. Sci. Technol. 14 (5) (2003) R49.
[16] J.M. Corres, I.R. Matias, I.D. Villar, F.J. Arregui, Design of pH sensors in long-period fiber gratings using polymeric nanocoatings, IEEE Sens. J. 7 (3) (2007) 455–463.
[17] M. Consales, G. Quero, S. Zuppolini, L. Sansone, A. Borriello, M. Giordano, A. Venturelli, M.P. Costi, M. Santucci, A. Cusano, Long period fiber grating biosensor for the detection of drug resistant bacteria: the 'OPTObacteria' project, Third Mediterranean Photonics Conference (2014) 1–3.
[18] M. Janczuk-Richter, M. Dominik, E. Roźniecka, M. Koba, P. Mikulic, W.J. Bock, M. Łoś, M. Śmietana, J. Niedziółka-Jönsson, Long-period fiber grating sensor for detection of viruses, Sens. Actuators B 250 (2017) 32–38.
[19] S. Korposh, S. James, R. Tatam, S.-W. Lee, Optical Fibre Long-Period Gratings Functionalised with Nano-Assembled Thin Films: Approaches to Chemical Sensing, (2013).
[20] S. Korposh, S.-W. Lee, S.W. James, R.P. Tatam, Refractive index sensitivity of fibre-optic long period gratings coated with SiO 2 nanoparticle mesoporous thin films, Meas. Sci. Technol. 22 (7) (2011) 075208.
[21] Y. Li, H.J. Schluesener, S. Xu, Gold nanoparticle-based biosensors, Gold Bull. 43 (1) (2010) 29–41.
[22] L. Marques, F.U. Hernandez, S.W. James, S.P. Morgan, M. Clark, R.P. Tatam, S. Korposh, Highly sensitive optical fibre long period grating biosensor anchored with silica core gold shell nanoparticles, Biosens. Bioelectron. 75 (2016) 222–231.
[23] J.M. Pingarrón, P. Yáñez-Sedeño, A. González-Cortés, Gold nanoparticle-based electrochemical biosensors, Electrochim. Acta 53 (19) (2008) 5848–5866.
[24] M. Gambhir, S. Gupta, Review of turn around point long period fiber gratings, J. Sens. Technol. 05 (04) (2015) 81–89.
[25] J. Hromadka, R. Correia, S. Korposh, Fabrication of fiber optic long period gratings operating at the phase matching turning point using an amplitude mask, Sixth European Workshop on Optical Fibre Sensors (EWOFS'2016), SPIE, 2016 p. 99160Y.
[26] L. Viau, T. Vrlinic, F.E. Jurin, B. Lakard, Elaboration of thin colloidal silica films with controlled thickness and wettability, C.R. Chim. 19 (5) (2016) 665–673.
[27] I.D. Villar, I.R. Matías, F.J. Arregui, P. Lalanne, Optimization of sensitivity in Long Period Fiber Gratings with overlay deposition, Opt. Express 13 (1) (2005) 56–69.
[28] P.C. Weber, D.H. Ohlendorf, J.J. Wendoloski, F.R. Salemme, Structural origins of high-affinity biotin binding to streptavidin, Science 243 (4887) (1989) 85–88.
[29] J. Wong, A. Chilkoti, V.T. Moy, Direct force measurements of the streptavidin–biotin interaction, Biomol. Eng. 16 (1–4) (1999) 45–55.
[30] M. Srisa-Art, E.C. Dyson, A.J. deMello, J.B. Edel, Monitoring of real-time streptavidin-biotin binding kinetics using droplet microfluidics, Anal. Chem. 80 (18) (2008) 7063–7067.
[31] G. Kemmer, S. Keller, Nonlinear least-squares data fitting in Excel spreadsheets, Nat. Protoc. 5 (2) (2010) 267–281.
[32] D.G. Kinniburgh, General purpose adsorption isotherms, Environ. Sci. Technol. 20 (9) (1986) 895–904.
[33] F.J. Arregui, Sensors Based on Nanostructured Materials, Springer, New York, London, 2011.
[34] R. Saber, S. Sarkar, P. Gill, B. Nazari, F. Faridani, High resolution imaging of IgG and IgM molecules by scanning tunneling microscopy in air condition, Scientia Iranica 18 (6) (2011) 1643–1646.
[35] D.M. Czajkowsky, Z. Shao, The human IgM pentamer is a mushroom-shaped molecule with a flexural bias, Proc. Natl. Acad. Sci. U. S. A. 106 (35) (2009) 14960–14965.
[36] W.R. Wong, O. Krupin, S.D. Sekaran, F.R. Mahamd Adikan, P. Berini, Serological diagnosis of dengue infection in blood plasma using long-range surface plasmon waveguides, Anal. Chem. 86 (3) (2014) 1735–1743.
[37] D. Atias, Y. Liebes, V. Chalifa-Caspi, L. Bremand, L. Lobel, R.S. Marks, P. Dussart, Chemiluminescent optical fiber immunosensor for the detection of IgM antibody to dengue virus in humans, Sens. Actuators B: Chem. 140 (1) (2009) 206–215.
[38] J. Choi, A.W. Gani, D.J.B. Bechstein, J.-R. Lee, P.J. Utz, S.X. Wang, Portable, one-step, and rapid GMR biosensor platform with smartphone interface, Biosens. Bioelectron. 85 (2016) 1–7.
[39] M.F. Goldstein, A.L. Goldstein, E.H. Dunsky, D.J. Dvorin, G.A. Belecanech, K. Shamir, Selective IgM immunodeficiency: retrospective analysis of 36 adult patients with review of the literature, Ann. Allergy Asthma Immunol. 97 (6) (2006) 717–730.
[40] M.F. Goldstein, A.L. Goldstein, E.H. Dunsky, D.J. Dvorin, G.A. Belecanech, K. Shamir, Pediatric selective IgM immunodeficiency, Clin. Dev. Immunol. 2008 (2008) 624850.
[41] J. Hromadka, S. Korposh, M.C. Partridge, S.W. James, F. Davis, D. Crump, R.P. Tatam, Multi-parameter measurements using optical fibre long period gratings for indoor air quality monitoring, Sens. Actuators B 244 (2017) 217–225.

Dr Ricardo Goncalves Correia graduated in 2004 with a 5 year degree in Instrumentation and Industrial Quality Engineering from the Superior Institute of Engineering of Porto. In 2005 he joined the Engineering Photonics group at Cranfield University to pursuit a PhD in the development of a fibre optic pore pressure sensor employing Fibre Bragg Gratings. As a post-doctoral fellow he has further developed interferometric and Bragg grating based fibre optic sensors for civil and aerospace engineering applications. In 2015 he joined the UoN where he is currently working on the development of fibre optic sensors for healthcare applications.

Professor Stephen P. Morgan is Professor of Biomedical Engineering at UoN. Since 1992, he has investigated novel optical techniques for imaging and spectroscopy of tissue using laser Doppler flowmeter y, acousto-optic imaging and hyperspectral imaging. His research involves the development of devices to monitor the microcirculation specifically in tissue breakdown and wound healing. For example, he currently developing a novel endotracheal tube that can monitor the microcirculation at the cuff/trachea interface. Recent work involves the integration of optical fibre sensors into textiles. These sensing systems, incorporated into garments can monitor pressure, temperature and the microcirculation.

Dr Serhiy Korposh received both his bachelor and master degrees in 2001 and 2002 respectively in physics from Uzhgorod National University, Transcarpathia (Ukraine) and Ph.D. degree from Cranfield University in 2007. He worked as a postdoctoral researcher on development of the novel materials for chemical sensors in the Graduate School of Environmental Engineering of the University of Kitakyushu from 2008 to 2012. From 2012–2013 he worked as a research fellow in the Department of Engineering Photonics, Cranfield University. He is currently Lecturer at the University of Nottingham. His research interest lies in the field of application and development of fibre-optic chemical sensors modified with the sensitive materials.